Dynamic microtubules and specification of the zebrafish embryonic axis

Suresh Jesuthasan* and Uwe Strähle†

Background: The zebrafish is emerging as an important genetic system for the study of vertebrate development, and many zygotic mutations affecting embryogenesis have been isolated. The early events in development are under the control of maternal genes but are relatively unexplored. Here, the process of axis specification is investigated.

Results: The vegetal pole of the zygote transiently contains a dense array of parallel microtubules, while microtubules near the equator are disorganized. Irradiation of the zygote with ultraviolet light disrupts the formation of the vegetal microtubule array and causes loss of the axis; brief treatment with nocodazole at this stage also causes defects in the axis. During cleavage stages, yolk cortical microtubules reorganize to form arrays that apparently extend from marginal blastomeres. Prolonged exposure to cold (18 °C) or incubation in nocodazole prior to the 32-cell stage disrupts cortical microtubules and causes premature formation of the yolk syncytial layer; these treatments also prevent formation of an axis, as indicated by the absence of *goosecoid* and *forkhead2* expression and of translocation of β-catenin into nuclei. Cortical microtubule arrays are required for the transport of particles from the vegetal hemisphere into marginal blastomeres, as shown by the movement of polystyrene beads; treatments that prevent axis formation also prevent the entry of beads into blastomeres.

Conclusions: To form an organizer, zebrafish blastomeres appear to require substances which are transported from the vegetal hemisphere of the yolk cell by cortical microtubules. Initial asymmetry appears dependent on an array of parallel microtubules at the vegetal pole.

Addresses: *Max-Planck-Institut für Entwicklungsbiologie, Spemannstraβe 35/I, 72076 Tübingen, Germany. †IGBMC, CNRS/INSERM/ULP, BP163, 67404 Illkirch, France.

Correspondence: Suresh Jesuthasan
E-mail: sj@fserv1.mpib-tuebingen.mpg.de

Received: 15 April 1996
Revised: 19 August 1996
Accepted: 25 October 1996

Published: 18 December 1996
Electronic identifier: 0960-9822-007-00031

Current Biology 1996, 7:31–42

Background

Specification of the dorsoventral axis occurs early in embryonic development. In vertebrates, establishment of this axis leads to the formation of an organizer, which is required for various events such as specification of different mesodermal cell types and induction of neural tissue. In teleosts, the organizer corresponds to the shield [1], in amphibians to the dorsal lip [2], in chick to Hensen's node [3] and in mouse to the node [4]. The initial steps in the formation of an organizer are obscure in all vertebrates except for amphibians; in this case, the cylindrical symmetry of the egg is broken by sperm entry, leading to rotation of the cortex towards the future dorsal side of the embryo [5,6].

How is the dorsoventral axis established in the zebrafish? The zebrafish zygote, whose animal–vegetal axis is easily visible minutes after fertilization with the formation of a blastodisc at the animal pole, appears radially symmetrical when viewed from the animal pole. Unlike amphibians, there is no pigmentation that demarcates the future dorsal side, nor has any cortical rotation been reported [7]. Morphological radial symmetry is broken by the first cleavage, but the dorsoventral axis does not consistently correlate with this cleavage plane in zebrafish [8–11] or other teleosts [12,13]. Thus, formation of dorsoventral asymmetry is unlikely to be caused by the unequal partitioning of a cytoplasmic factor during cytokinesis of early blastomeres. Consistent with this idea, *Fundulus* embryos develop normally when one blastomere is removed at the 2-cell or 4-cell stage [14,15]. As blastomeres divide further, they form a mound of cells at the animal pole, and the embryo appears radially symmetrical again. Although there is some subtle morphological asymmetry at 30 % epiboly in the zebrafish [16], it is only at the start of gastrulation (50 % epiboly) that the dorsoventral axis becomes obvious with formation of the shield.

At the molecular level, radial symmetry of the zebrafish embryo seems to be lost at the cleavage stage. Genes which are expressed in the shield, such as *goosecoid* [17] and *forkhead2* ([18] and J. Odenthal, personal communication), are already located asymmetrically within the blastoderm at the sphere stage. Earlier still, from the 32-cell

stage onwards, exposure to lithium chloride causes the formation of dorsalized embryos [17]. As lithium ions may inhibit phosphoinositide metabolism (reviewed in [19]) or glycogen synthase kinase-3β [20], this finding indicates that the young embryo contains some dorsoventral asymmetry that is mediated by the phosphoinositol or the Wingless/β-catenin signal-transduction pathways.

At the very early stages of zebrafish development, dorsoventral polarity may not exist in the blastoderm but in the yolk cell. In other teleosts, at least, the yolk cell is required initially for the formation of an organizer. When *Fundulus* blastoderms were cultured after isolation from the yolk cell, no axial structures formed if the separation was performed prior to the 32-cell stage, whereas blastoderms

Figure 1

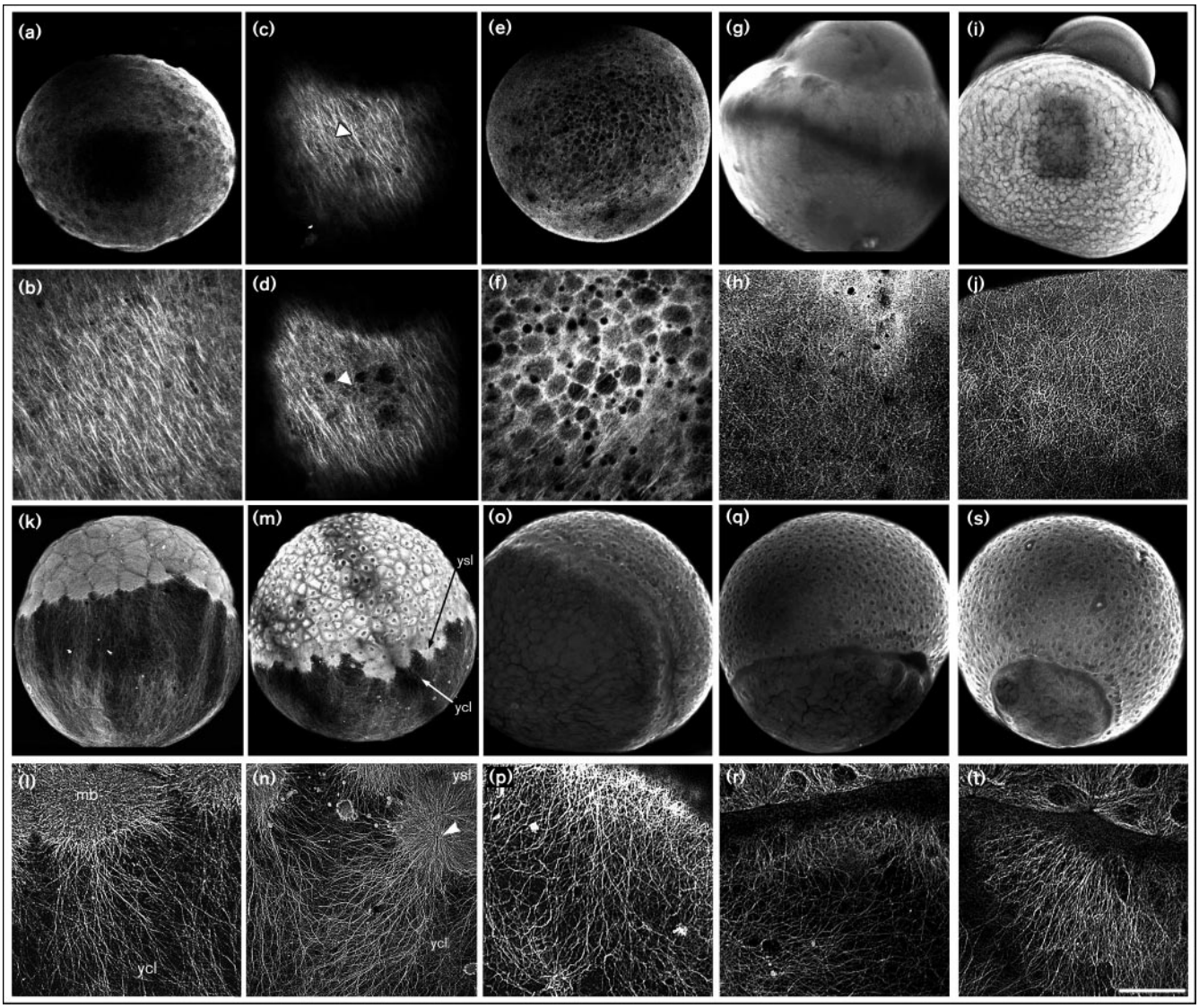

Microtubules in the yolk cortex from the 1-cell stage to 90 % epiboly. (a) Vegetal-pole view of a zygote 20 min post-fertilization. (b) At high magnification, many short fibrils are visible, aligned with one another. The region imaged at high magnification is the bleached region in (a). (c,d) Single optical sections of the same embryo. At a shallow focal plane (c), aligned fibrils are visible, whereas 6 μm deeper (d), fibrils with a different orientation are detectable. The arrowheads indicate equivalent positions in each image. (e,f) Vegetal-pole view of an embryo 30 min post-fertilization. A sparse array of parallel microtubules is visible, slightly offset from the vegetal pole, which is located near the top of the frame. (g,h) Lateral view of an embryo, 30 min post-fertilization, with short, unaligned microtubules near the blastoderm. (i,j) A 4-cell embryo, with unaligned microtubules at the equator. (k,l) At the 256-cell stage, aligned microtubules are visible, apparently extending from marginal blastomeres (mb) into the yolk cytoplasmic layer (ycl). (m,n) An embryo at the high-blastula stage with many microtubules adjacent to the yolk syncytial layer (ysl). The arrowhead indicates an aster. Embryos at 50 % (o,p), 70 % (q,r) and 90 % (s,t) epiboly have long microtubules in the yolk cytoplasmic layer. Scale bar in (t) represents 200 μm for (a,e,g,i,k,m,o,q,s) and 40 μm for (b–d,f,h,j,l,n,p,r,t). All high-magnification images, except for (c,d), have been crispened.

isolated at the 32-cell stage or later contained notochord cells [21]. Similarly, isolated loach blastoderms formed well-differentiated structures only when they were separated from the yolk cell several hours after fertilization [22], and removal of the yolk cell from goldfish embryos before the 8-cell stage prevented the formation of notochord [23]. The formation of an organizer in these teleosts therefore seems to require molecules in the yolk cell that are subsequently transported to the blastoderm [21]. How these molecules are transported and whether such a transfer is required in the zebrafish are not known. In the zebrafish, at least some of the molecules involved in establishing dorsoventral polarity appear to be sensitive to ultraviolet (UV) light, because irradiation of the zygote can prevent formation of a morphologically distinct axis [24]. The mechanism by which asymmetry is generated remains unclear, however, as the targets of UV irradiation at this stage are not known.

In this study, we provide evidence that specification of the dorsoventral axis in the zebrafish embryo is dependent on the transfer of substances from the yolk cell to blastomeres, by cortical microtubules which extend from marginal blastomeres to the vegetal hemisphere [24,25]. The establishment of asymmetry in the zygote is shown to depend on a parallel array of microtubules at the vegetal pole.

Results

The distribution of microtubules in the yolk cell

The zebrafish yolk cell was examined using immunofluorescence and confocal microscopy, and was found to contain cortical microtubules whose distribution and organization changed during early cleavage stages. Approximately 20 minutes after fertilization (0.44 normalized time; the time for the first cleavage is 45 minutes, and the time for subsequent cleavages is 15 minutes [26]), filaments at the vegetal pole formed a parallel array (Fig. 1a,b), thereby breaking the radial symmetry of the embryo; no array was detected in embryos fixed 10 minutes post-fertilization. The array was located at a shallow position (Fig. 1c,d), less than 2 μm from the surface (as determined by *xz* sectioning) and was found only at the vegetal pole. Microtubules adjacent to the blastodisc and at the equator were disorganized. At 30 minutes post-fertilization, a number of aligned fibrils could be seen offset from the vegetal pole (Fig. 1e,f), whereas fibrils near the blastodisc were not aligned (Fig. 1g,h). During and after first cleavage, aligned fibrils were not detected at the vegetal pole. At the 4-cell stage, short fibrils with no obvious orientation were seen at the equator (Fig. 1i,j). In embryos examined from the 32-cell stage up to the 256-cell stage, long arrays of microtubules, apparently emanating from marginal blastomeres, were visible (Fig. 1k,l). These arrays extended beyond the equator.

At all subsequent stages of development, the yolk cytoplasmic layer (yolk cortex) contained cortical microtubules that continued to form long arrays (Fig. 1m–t). The length of these microtubules was measured at different stages (Fig. 2). This quantitation suggests that microtubules in the yolk cortex at the 1-cell to 4-cell stages are considerably shorter than those found at later stages.

Figure 2

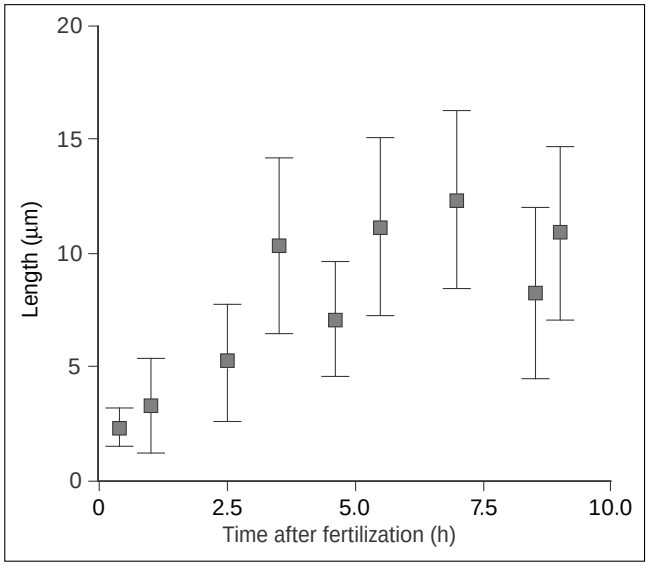

Quantitation of length of microtubule fibrils/bundles in the yolk cell, as a function of time. Microtubule fibrils/bundles are initially short and increase in length during first few hours of development. Bars indicate standard deviation.

The effects of UV irradiation on early stage embryos

UV treatment prior to the first cleavage has been shown to result in embryos which lack an obvious body axis [24]. In addition, UV light was found to retard epiboly, irrespective of the time of application. To document in more detail the effects of UV light on early development, embryos were irradiated after fertilization *in vitro* (Table 1), and were

Table 1

Effects of UV irradiation prior to the first cleavage.

	Time of UV treatment		
	10 min post-fertilization	25 min post-fertilization	Untreated
Appearance of embryo			
Axis absent	7	11	0
Epiboly incomplete*	10	18	0
Normal	0	0	47
Survivors†	36 %	69 %	82 %

Embryos were irradiated for 90 sec and assessed for the presence of an axis when untreated siblings reached 100 % epiboly. The proportion of embryos lacking a morphological axis is similar to those lacking expression of *axial* and *sonic hedgehog*. *Embryos with incomplete epiboly include those in which blastoderms pinched off from the yolk (see [25]). †The viability count includes unfertilized eggs.

Figure 3

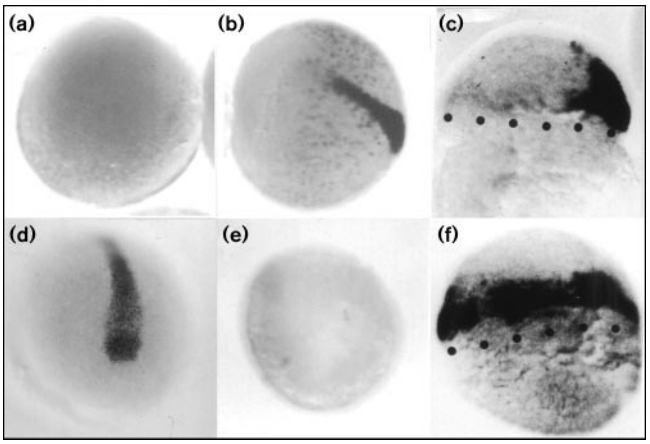

Effects of UV irradiation on gene expression in the dorsal midline. (a) *axial* expression is undetectable in this embryo, which had been irradiated 10 min after fertilization. (b) An unirradiated sibling, with *axial* expression in the axis and in scattered cells in the hypoblast. (c) Expression of *axial* in an embryo irradiated during early cleavage. (d) Expression of *sonic hedgehog* in an untreated embryo at 75 % epiboly. (e) A sibling, which had been irradiated 10 min after fertilization, lacks detectable *sonic hedgehog* expression. (f) Expression of *notail* in an early-UV-irradiated embryo. Dots indicate the blastoderm margin.

analyzed with molecular probes for the organizer region. The expression of *axial* mRNA, which is usually found in midline cells [27], was not detectable in a subset of embryos exposed to UV light 10 minutes after fertilization and examined at the 40 % epiboly stage (Fig. 3a). Untreated embryos of the same age had progressed further through epiboly (75 %), and were all labelled strongly with the *axial* probe (Fig. 3b). Exposure to UV light *per se* did not abolish *axial* expression, because all embryos that were irradiated during early cleavage stages expressed *axial* strongly (Fig. 3c). Another marker for the axis, *sonic hedgehog* [28], was also not detected in a subset of early UV-irradiated embryos (compare Fig. 3d,e). The *notail* mRNA, which is expressed throughout the mesoderm and in several other cell types [29], was present in the blastoderm margin of embryos derived from early UV-treated zygotes (Fig. 3f).

In order to determine whether early UV treatment caused a loss of the vegetal array of microtubules, embryos that had been irradiated 10 minutes after fertilization were fixed and then labelled with an antibody to β-tubulin. Embryos fixed 10 minutes after irradiation (20 minutes post-fertilization) did not contain a vegetal array (Fig. 4a; 6 embryos imaged), whereas 3 out of 10 embryos fixed 20 minutes after irradiation contained sparsely aligned fibrils (Fig. 4b,c). To determine whether loss of the axis was due solely to a transient loss of microtubules, embryos were incubated in the microtubule-depolymerizing drug nocodazole [30,31] at a concentration of 0.1 μg ml^{-1}, for 4 minutes at 5, 10 or 15 minutes post-fertilization. Only early treatment caused loss of the axis (Fig. 5). Transient treatment with this dose after the first cleavage did not cause any defect in the axis.

Cold treatment inhibits epiboly and axis specification, and induces formation of an enlarged yolk syncytial layer

Microtubules are known to depolymerize at low temperatures [32,33], and cleavage-stage embryos developed abnormally when grown at 18 °C (Fig. 6a). We therefore examined the effect of cold on embryos of different stages. Cold treatment of embryos at the 256-cell stage or earlier always led to the formation of an enlarged yolk syncytial layer, whereas treatment at or after the 512-cell stage, which is when the yolk syncytial layer normally forms, did not. In embryos cooled at the 1-cell stage, no cells were visible even after 4 hours, although many nuclei could be seen within the large cytoplasm (Fig. 6b). In embryos cooled from the 2-cell stage, distinct cells formed, always in pockets. The large cytoplasm, which was always multinucleate (Fig. 6c), was continuous with the yolk cytoplasmic layer, as demonstrated by the spreading of TRITC-dextran that had been injected into this region. The size of this abnormal yolk syncytial layer depended on the time of treatment: the earlier the treatment, the larger the syncytium.

Figure 4

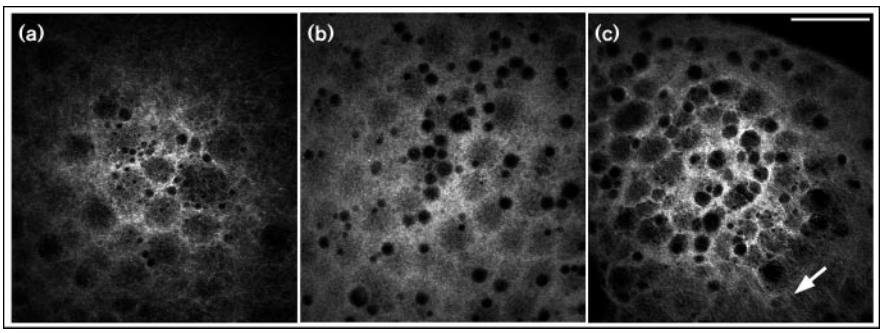

Microtubules in UV-irradiated embryos. (a) Vegetal pole region of an embryo fixed 10 min after irradiation. Only unaligned microtubules are detectable. (b) Vegetal pole region of an embryo fixed 20 min after irradiation. No array is detectable. (c) Another embryo fixed 20 min after irradiation. A sparse microtubule array (arrow) can be seen. Scale bar = 50 μm.

After 24 hours incubation at 18 °C, embryos cooled at the 2- to 16-cell stages still contained pockets of cells and an enlarged yolk syncytium. Epiboly was not evident, and no gastrulation occurred (Table 2; Fig. 6d). Embryos cooled at the 32- to 128-cell stages did not complete epiboly, but underwent some gastrulation, as indicated by the formation of a distinct hypoblast and epiblast (Fig. 6e). Embryos cooled at the 256-cell stage onwards could complete epiboly and form a distinct axis, but their yolk cells were elongated (Fig. 6f). In contrast, embryos cooled from the sphere stage (4 hours post-fertilization) had spherical yolk cells after the completion of epiboly. The detrimental effect of cold is thus highly stage-dependent: early exposure to cold triggers the formation of an enlarged yolk syncytial layer, prevents gastrulation and strongly retards epiboly; later cooling does not prevent gastrulation but still inhibits epiboly; with even later cooling, normal development can occur.

Figure 5

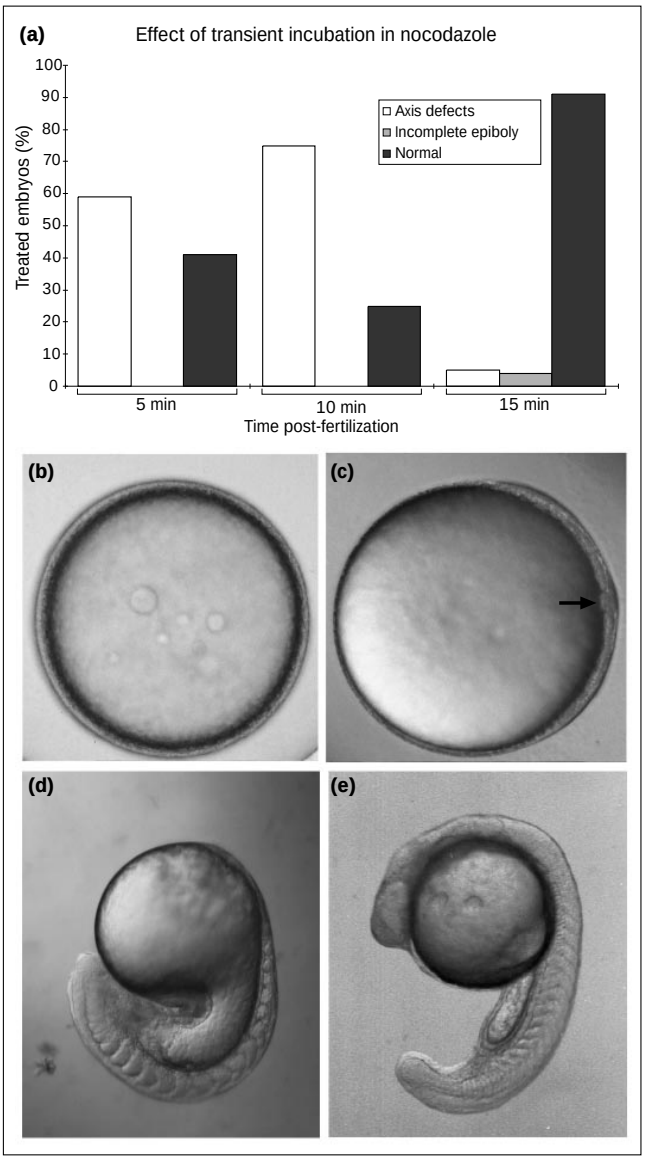

Transient nocodazole treatment early in the first cell cycle disrupts the formation of an axis. (a) Graph showing the effects of 4 min incubation in 0.1 μg ml^{-1} nocodazole at 5 min (n = 44), 10 min (n = 75) and 15 min (n = 56) after fertilization *in vitro*. Treated embryos were examined when untreated siblings had reached 100 % epiboly, and at 24 h post fertilization. Embryos with axis defects include those completely lacking an axis (as in (b)), and those with anterior truncations (as in (d)). (b) An embryo which had been transiently incubated in 0.1 μg ml^{-1} nocodazole 10 min post-fertilization, viewed from the vegetal pole, with the equator in focus. No axis is visible. (c) An untreated sibling, also viewed from the vegetal pole, with a well-formed axis. The notochord primordium is indicated. (d) Anterior truncation, as seen in approximately 50 % of the embryos transiently treated with 0.1 μg ml^{-1} nocodazole 5 or 10 min post-fertilization. This embryo lacks eyes, anterior neural tube, otic vesicles and notochord. (e) An untreated embryo 24 h post-fertilization.

Early cold treatment prevents the formation of an organizer

Embryos cooled from early cleavage stages were analyzed further to determine why they failed to gastrulate. An antibody to Notail [29] was used to assess whether the blastoderm had differentiated. All treated embryos, including those cooled continuously from the 4-cell and 8-cell stages, contained Notail protein. Initially, labelling was seen in deep cells, as well as in the enlarged syncytium and enveloping layer (Fig. 7b,c); after 24 hours, only deep cells were labelled (Fig. 7d). To assess whether the failure to gastrulate was correlated with the absence of an organizer, embryos were analyzed with probes to two genes expressed in the organizer, *goosecoid* [17] and *forkhead2* ([18] and J. Odenthal, personal communication). *Goosecoid* was detected in a restricted region of the blastoderm in all embryos which had been cooled from the 128-cell and 256-cell stages (Fig. 7e; n = 22), and in lower amounts in 8 out of 14 embryos cooled from the 32-cell and 64-cell stages. No labelling was found in embryos cooled from the 4-cell and 8-cell stages (Fig. 7f; n = 28). *Forkhead2*, which is normally expressed earlier than *goosecoid* — initially in the entire yolk syncytial layer and then in the dorsal region of the blastoderm margin — was detected in all embryos cooled from the 32-cell to 256-cell stages (Fig. 7g; n = 32), but not in embryos cooled

Table 2

Effects of constant incubation at 18 °C on survival and epiboly.

Stage cooled	Survivors after 24 h (%)	Embryos that completed epiboly (%)
1-cell	100 (n = 20)	0
2-cell	74 (n = 27)	0
4-cell	60 (n = 00)	0
8-cell	75 (n = 65)	0
16-cell	39 (n = 31)	0
32-cell	6 (n = 35)	0
128-cell	40 (n = 20)	0
256-cell	85 (n = 20)	65
512-cell	94 (n = 18)	82
1 000-cell	88 (n = 24)	95
Sphere	94 (n = 18)	94

Figure 6

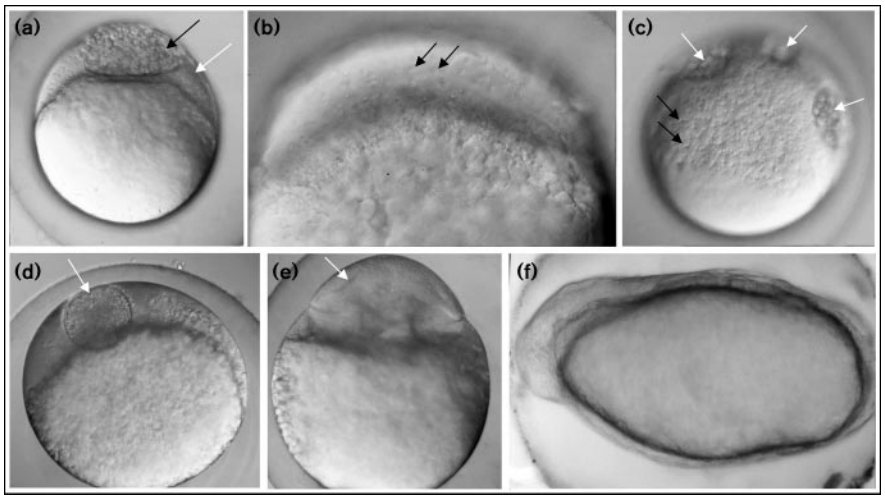

Effects of incubating embryos at 18 °C. (a) An 8 h old embryo which had been cooled at the 2-cell stage. An enlarged yolk syncytial layer (white arrow) and a pocket of cells (black arrow) are visible at the animal pole. (b) This embryo contains multiple nuclei (arrows) in a syncytium, 8 h after being cooled at the 1-cell stage. (c) An 8 h embryo which had been cooled at the 8-cell stage. Multiple nuclei (black arrows) are visible in the yolk syncytial layer. Three pockets of cells (white arrows) have formed in this case. (d) An embryo which had been cooled at the 4-cell stage, after 24 h. The enlarged syncytial layer and pocket of cells (arrow) remain at the animal pole. (e) An embryo which had been cooled at the 32-cell stage, after 24 h. Gastrulation movements have occurred, so that two distinct cell layers have formed. The arrow indicates the separation between the epiblast and hypoblast. (f) A 24 h-old embryo, which had been cooled at the 512-cell stage. Epiboly is complete and somitogenesis is under way, but the yolk has elongated abnormally. All embryos are shown in lateral view, except in (c), where the embryo was mounted approximately 45 ° from the animal-pole-up position.

from the 4-cell or 8-cell stages (Fig. 7h; $n = 22$). Hence, embryos which were cooled early, and which failed to gastrulate, lacked expression of organizer genes, implying that the treatment prevents the formation of an organizer.

An earlier marker of dorsoventral asymmetry, translocation of β-catenin into nuclei, was also examined. In zebrafish embryos, the nuclear translocation of β-catenin occurs first in a restricted number of nuclei in the yolk syncytial layer

Figure 7

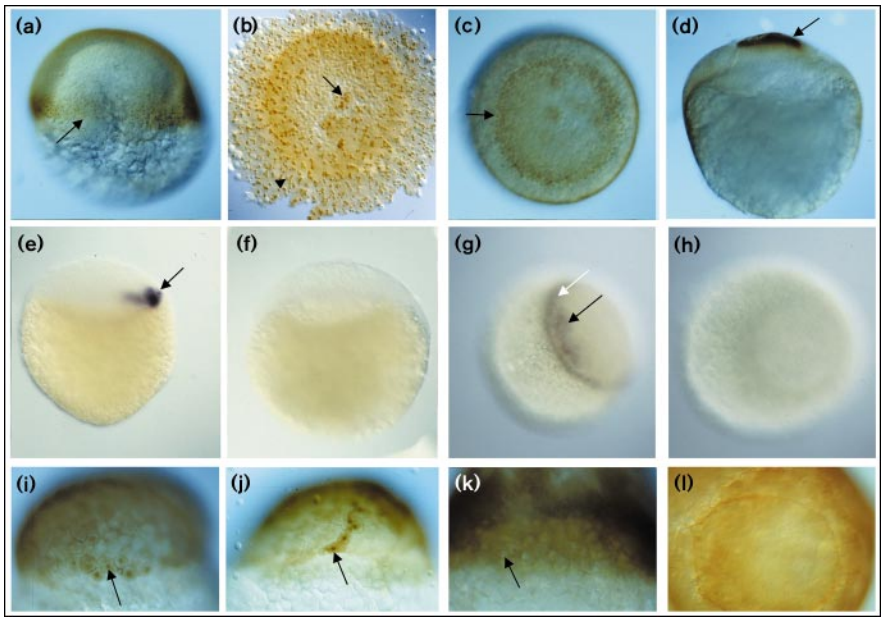

The expression of early differentiation and dorsal markers in untreated and cold-treated embryos. (a) Lateral view of an untreated embryo at 50 % epiboly, with Notail in nuclei of cells at the blastoderm margin (arrow). (b) In embryos cooled for 10 h at the 8-cell stage, nuclei of the enlarged yolk syncytial layer were labelled (arrowhead). Multinucleate cells near the animal pole (black arrow) were also labelled. This preparation was flattened after being isolated from the yolk; the ring of light brown staining indicates the blastoderm margin. (c) Animal-pole view of an embryo cooled at the 32-cell stage, with a ring of Notail-positive cells at the margin of the blastoderm (arrow). (d) A 24 h-old embryo that had been cooled since the 4-cell stage. Notail is found only in cells of the blastoderm, which is here confined to the animal pole (arrow). (e) Expression of *goosecoid* (arrow) in an embryo which had been cooled at the 128-cell stage. (f) No *goosecoid* expression was detected in this embryo, which had been cooled at the 8-cell stage. (g) *Forkhead2* expression in the syncytial layer (white arrow) and blastoderm (black arrow) of an embryo cooled at the 32-cell stage. (h) An embryo which had been cooled at the 4-cell stage, with no detectable *forkhead2* mRNA. (i) β-catenin is translocated to the nuclei of a restricted number of cells (arrow) in the blastoderm of untreated embryos at the high blastula stage. (j) An embryo cooled at the 128-cell stage for 2.2 h, with nuclei containing β-catenin (arrow). Embryos cold-treated at the 8-cell stage, for 4 h (k) or 6 h (l), have no nuclear translocation of β-catenin. The arrow in (k) indicates an unlabeled nucleus in the syncytial layer; (l) shows an optical section taken from the animal pole, at the level of the yolk syncytial layer. The ring of label indicates an association of β-catenin with the double membrane separating the pocket of blastomeres from the enlarged yolk syncytial layer.

at the high-blastula stage [34]. Subsequently, β-catenin is translocated into the nuclei of a subset of deep cells in the dorsal region (Fig. 7i). In embryos fixed 3.2 and 2.2 hours after being cooled at the 32-cell and 128-cell stages, respectively, β-catenin was found inside nuclei in a restricted region in the blastoderm (Fig. 7j) or in the yolk syncytial layer. In contrast, embryos fixed 4 hours (Fig. 7k) or 6 hours (Fig. 7l) after being cooled at the 8-cell stage did not have any labelled nuclei in the syncytial layer or in the blastoderm. Hence, asymmetry in the yolk syncytial layer is also lost in embryos exposed to cold at early cleavage stages.

The effects of cold treatment are due to the disruption of microtubules

To determine whether the defects caused by exposure to cold resulted from the disruption of microtubules, embryos were incubated continuously in nocodazole. In 0.5, 1, 5 or 10 μg ml^{-1} nocodazole, blastomeres stopped dividing and became rounded (20 embryos at the 32-cell to 64-cell stages were incubated at each concentration; Fig. 8a). Treated embryos formed an enlarged syncytial layer between the yolk and blastoderm, which remained at the animal pole even when control embryos had reached the 70 % epiboly stage. Cell division was not blocked completely in embryos incubated in 0.1 μg ml^{-1} nocodazole, but an enlarged syncytium, similar to that in embryos treated with higher doses of nocodazole, did form (Fig. 8b; n = 20, at the 64-cell stage). The blastoderm remained at the animal pole even when untreated siblings had reached 100 % epiboly. When

Figure 8

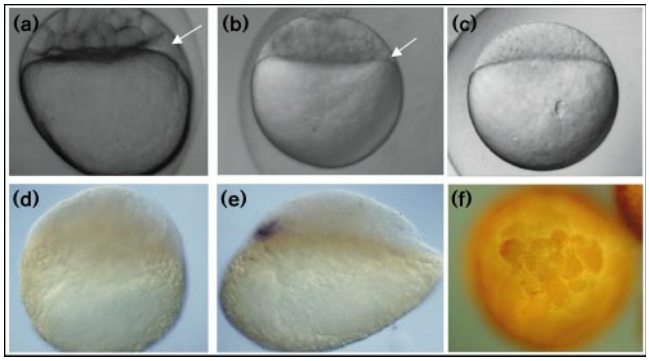

Effects of incubating cleavage-stage embryos in nocodazole. Embryos in (a–c) are shown 5 h after treatment. (a) An embryo which had been incubated at the 32-cell stage in 10 μg ml^{-1} nocodazole. Cell and nuclear division are arrested. An enlarged yolk syncytial layer has formed (arrow). (b) An embryo which had been incubated in 0.1 μg ml^{-1} nocodazole at the 64-cell stage. Cytokinesis of deep cells has not been blocked, but an enlarged yolk syncytial layer has formed (arrow). (c) An embryo which had been incubated in 0.1 μg ml^{-1} nocodazole at the 1-cell stage, with a large syncytium and no blastomeres. The irregularities are nuclei. (d) *Goosecoid* mRNA is not detectable in this 6 h embryo, which had been incubated in 0.1 μg ml^{-1} nocodazole from the 16-cell stage; (e) a sibling treated at the 32-cell stage has *goosecoid* mRNA in a restricted region of the blastoderm. (f) Animal-pole view of a 3 h embryo which had been incubated in 0.1 μg ml^{-1} nocodazole from the 16-cell stage, and then labelled with the anti-β-catenin antibody. No nuclear translocation of β-catenin is detectable. All embryos are shown in lateral view, except for the one in (f).

Figure 9

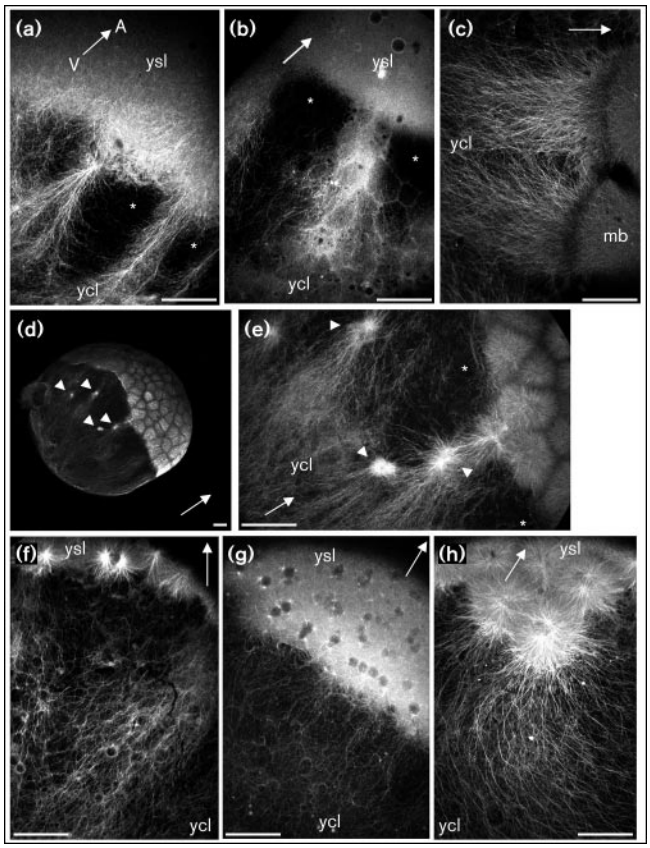

The distribution of microtubules in cold-treated and nocodazole-treated embryos. (a) An embryo which had been cold-treated at the 8-cell stage for 3 h. Microtubules are visible in the enlarged yolk syncytial layer (ysl) and in the yolk cytoplasmic layer (ycl). Large gaps (asterisks) separate microtubule arrays in the ycl. (b) An embryo incubated in 0.1 μg ml^{-1} nocodazole for 1 h from the 8-cell stage. Very few microtubules are visible in the yolk cortex, perhaps because treatment with this dose of nocodazole induces more depolymerization of microtubules than does incubation at 18 °C. Regions lacking microtubules are indicated by asterisks. (c) An untreated embryo at the 128-cell stage (1 h after the 8-cell stage). Large arrays of microtubules are visible adjacent to each marginal blastomere (mb), in the yolk cytoplasmic layer. (d,e) An embryo which had been incubated at 18 °C from the 8-cell stage, for 3 h. Microtubules in the yolk cortex appear to radiate from sites within ycl itself (arrowheads). Note the absence of microtubule arrays next to some 'blastomeres' (gaps indicated by asterisks). (f) An embryo cold-treated from the 8-cell stage for 5.5 h. Asters are visible in the enlarged syncytial layer, and relatively sparse microtubules are visible in the yolk cortex. (g) An embryo treated with 0.1 μg ml^{-1} nocodazole from the 8-cell stage for 3 h. Small asters are visible in the enlarged ysl, and relatively sparse microtubules can be seen in the yolk cortex. (h) An untreated embryo at the sphere stage, with a prominent microtubule array in the yolk cortex, and large asters in the syncytial layer. All embryos are shown in lateral view. The vegetal–animal (V–A) axis is indicated by the white arrow. Scale bar = 50 μm.

incubated in 0.05 μg ml^{-1} nocodazole at the 64-cell stage, embryos were indistinguishable from untreated siblings.

The effect of constant exposure to 0.1 μg ml^{-1} nocodazole was examined in embryos at different stages. As with exposure to 18 °C, incubation in 0.1 μg ml^{-1} nocodazole led to the formation of an enlarged yolk syncytial layer in embryos treated at the 256-cell stage and earlier, but not in embryos treated at the 512-cell stage or later. Embryos treated at the 1-cell stage formed only a large syncytium (Fig. 8c). To determine whether the partial disruption of microtubules at early cleavage stages was sufficient to prevent axis specification, the expression of *goosecoid* mRNA was examined in nocodazole-treated embryos. Embryos treated at the 8-cell and 16-cell stages did not express *goosecoid* (Fig. 8d); embryos treated at the 32-cell to 256-cell stages did express *goosecoid* (Fig. 8e), although expression was weak in 5 out of 10 embryos treated at the 32-cell stage. Treated embryos were also analyzed with the antibody to β-catenin: no nuclear translocation was found in the blastoderm or yolk syncytial layer of embryos treated at the 8-cell or 16-cell stages (Fig. 8f).

The distribution of microtubules was examined in embryos treated with cold or nocodazole. 3 hours after cold-treatment, arrays of microtubules were found in the yolk cortex, adjacent to the blastoderm (Fig. 9a). These microtubules were relatively well organized: they were aligned in the animal–vegetal axis, although there were large gaps between the arrays. A similar distribution was seen in embryos incubated for 1 hour in 0.1 μg ml^{-1} nocodazole (Fig. 9b). In contrast, untreated embryos of a

Figure 10

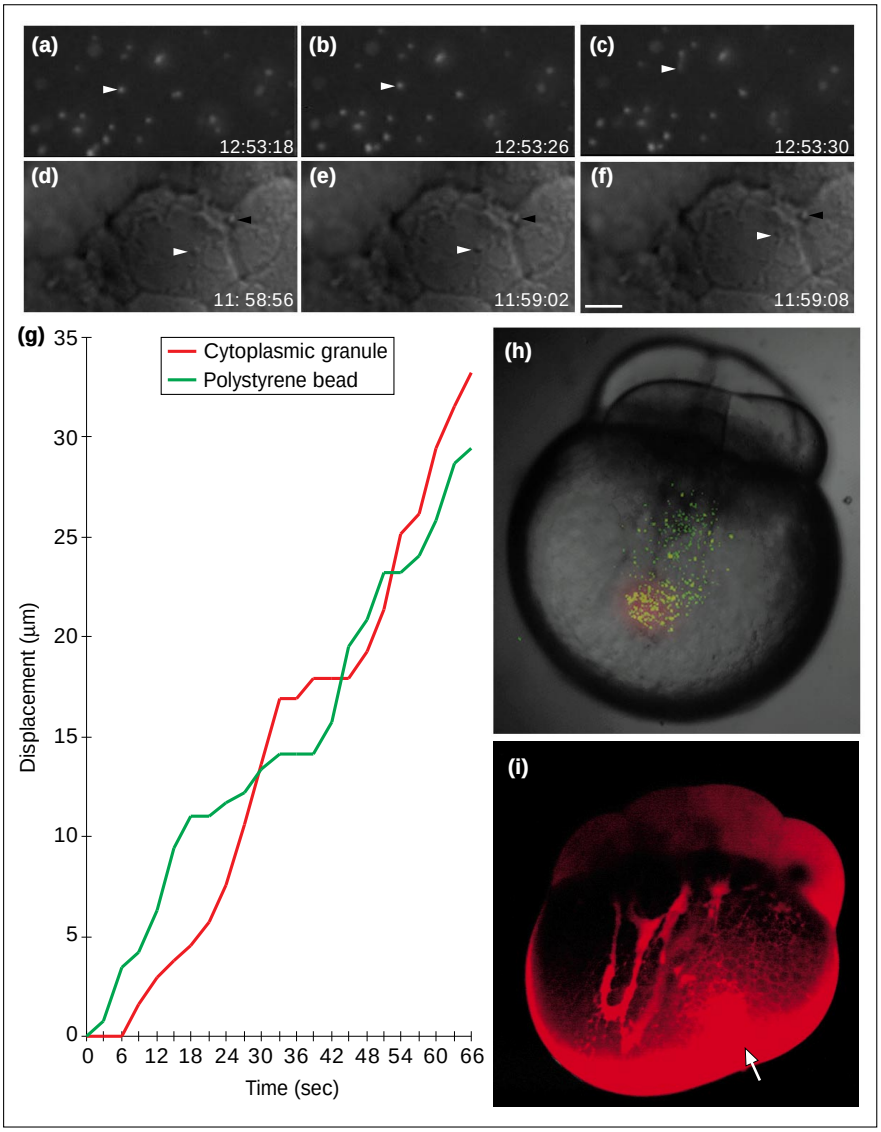

Movement in the yolk cytoplasmic layer. **(a–c)** Three frames from a time-lapse record of 0.2 μm polystyrene beads near the equator of an embryo at the 16-cell stage; beads had been injected near the vegetal pole at the 2-cell stage. The arrowhead indicates a bead that appears stationary between the first two frames and then moves towards the animal pole. **(d–f)** A cytoplasmic granule (white arrowhead) near the equator of an embryo at the 16-cell stage. No movement can be detected between the first two frames, but in the third frame the granule has moved towards the animal pole, and is closer to another granule (black arrowhead). Scale bar in (f) represents 10 μm (for panels a–f). **(g)** Plot of displacement *versus* time for a cytoplasmic granule (red line) and polystyrene bead (green line) in embryos at the 16-cell stage, showing the saltatory nature of movement. **(h)** An embryo which had been injected at the 4-cell stage, now with 8 cells. Beads have moved only towards the animal pole. Nile Red [47] was co-injected to label the injection site. **(i)** An embryo 15 min after TRITC–dextran was injected near the vegetal pole. The dye has spread uniformly from the injection site (arrow) and has already entered blastomeres.

similar age had closely spaced arrays that were in register with each marginal blastomere (Fig. 9c). Another irregularity found in cold-treated embryos was the presence of brightly labelled regions in the yolk cytoplasmic layer, from which numerous microtubules appeared to radiate (Fig. 9d,e). After approximately 5 hours incubation at 18 °C or 3 hours incubation in 0.1 μg ml^{-1} nocodazole, microtubules were still visible in the yolk cortex, but these were less dense than those seen in untreated embryos (compare Fig. 9f,g with 9h). These observations suggest that exposure to 18 °C or 0.1 μg ml^{-1} nocodazole causes a partial depolymerization of microtubules in addition to causing irregularities in their organization.

Microtubule-dependent particle movement in the yolk cytoplasmic layer

The formation of an axis in several other teleosts has been proposed to require the transport of substances from the yolk cell into the blastoderm (reviewed in [35]). To assess whether substances in the vegetal hemisphere of the zebrafish embryo could be transported to the blastoderm, 0.2 μm polystyrene beads were injected into the vegetal pole region at the 1-cell to 4-cell stage. Such beads have been shown to mimic the movement of organelles in a variety of cell types [36–38]. In the zebrafish yolk cortex, these beads moved with saltatory movement (Fig. 10a–c,g), as did endogenous cytoplasmic granules (Fig. 10d–g). Movement occurred only towards the animal pole (Fig 10h), in contrast to the uniform spread of dextran (Fig. 10i).

Polystyrene beads that were injected into the vegetal hemisphere were able to enter the blastoderm. Beads that moved between the yolk granules ended up in central blastomeres, whereas those that moved in the cortex entered marginal blastomeres (Fig. 11a–c). To confirm that bead movement in the cortex was dependent on microtubules, embryos

Figure 11

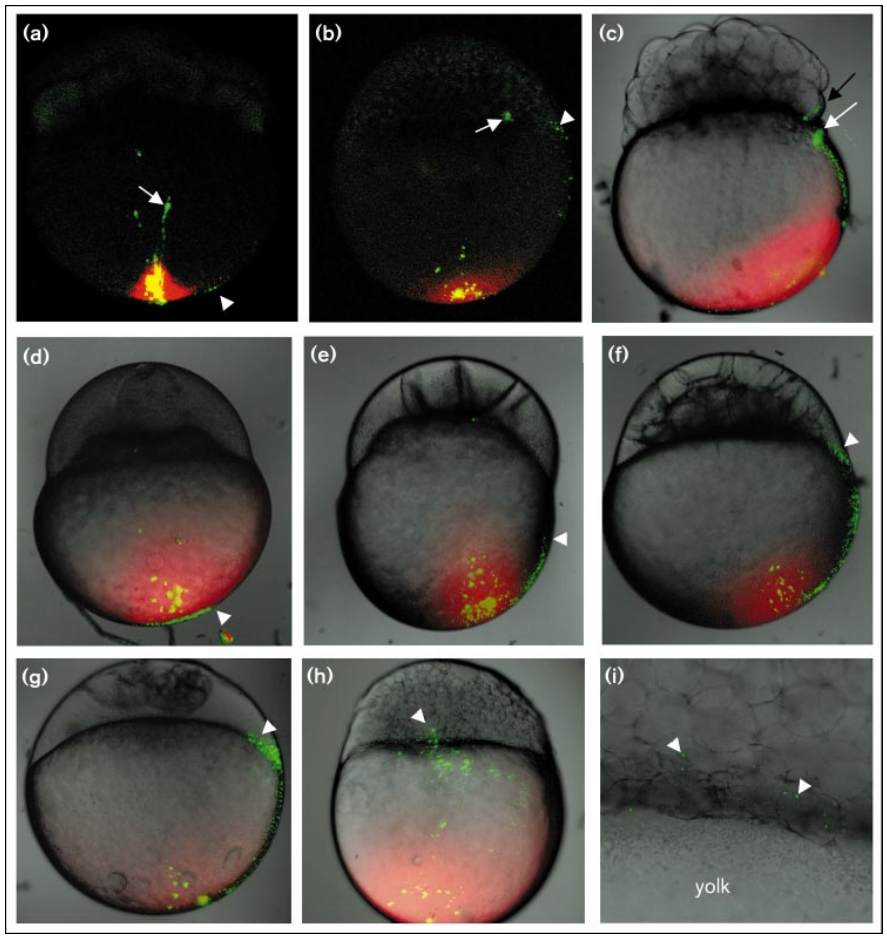

Polystyrene beads move from the vegetal hemisphere of early cleavage-stage embryos into the blastoderm. (a) At 15 min after injection at the 4-cell stage, beads (green) have moved away from the site of injection, which is marked by Nile Red. Some beads move along the cortex (arrowhead) while others move deep in the yolk cell (arrow), between yolk granules. (b) By 2.5 h later, beads can be seen in the blastoderm. Beads that travelled in the cortex end up in marginal blastomeres (arrowhead), while those that travelled between yolk granules end up in more central blastomeres (arrow). (c) Another embryo injected at the 2-cell stage, now at the 128-cell stage. Beads have entered a marginal blastomere (white arrow). Entry may have occurred at the 64-cell stage or earlier, as a cell higher up, which is likely to be a sister blastomere, also contains beads (black arrow). (d) An embryo incubated in 1 μg ml^{-1} nocodazole 5 min after injection at the 2-cell stage. Note the inhibition of cytokinesis; 1.5 h after injection, beads in the cortex still remain close to the site of injection; the arrowhead indicates the bead in the cortex closest to the animal pole. Beads deeper in the yolk, however, have moved and reached the large cytoplasm at the animal pole. (e) An embryo incubated in 1 μg ml^{-1} nocodazole 30 min after injection at the 2-cell stage; 1.5 h after injection, beads in the cortex (arrowhead) have not yet entered the blastoderm. (f) An embryo incubated in 1 μg ml^{-1} nocodazole 60 min after injection at the 2-cell stage; 30 min later, beads were found in the blastoderm (arrowhead). (g) An embryo incubated in 0.1 μg ml^{-1} nocodazole at the 8-cell stage, after injection at the 2-cell stage; 3 h later, beads were found in the enlarged yolk syncytial layer (arrowhead), but not in blastomeres. (h) An embryo incubated in 0.1 μg ml^{-1} nocodazole at the 128-cell stage, after injection at the 2-cell stage. Beads were found in blastomeres (arrowhead) and in the enlarged yolk syncytial layer when examined 1 h after treatment. (i) High-magnification view of a blastoderm margin of an untreated embryo at the high blastula stage, after injection at the 2-cell stage. Beads are visible inside deep cells (arrowheads). Embryos in all panels are in lateral view, with the animal pole upwards.

were incubated in 1 μg ml^{-1} nocodazole — a dose sufficient to stop microtubule-dependent processes such as cell and nuclear division. When nocodazole was applied 5 minutes after bead injection, beads in the cortex stopped moving, as evident from their presence only in the vegetal hemisphere when examined 1.5 and 4.5 hours after injection (Fig. 11d). When embryos were treated with nocodazole 30 minutes after injection, cortical beads only reached the equator (Fig. 11e); when incubated in nocodazole 60 minutes after injection, cortical beads reached the blastoderm (Fig. 11f). Similar results were obtained when embryos were treated with 10 μg ml^{-1} nocodazole, which has been shown to cause a complete loss of cortical microtubules [25].

To assess the behaviour of substances initially localized in the vegetal hemisphere in conditions under which an axis fails to form, the behaviour of polystyrene beads was examined in embryos treated with 0.1 μg ml^{-1} nocodazole or incubated at 18 °C. Neither treatment prevented the movement of beads in the cortex towards the animal pole, although the beads moved more slowly. In embryos treated with nocodazole immediately after injection at the 2-cell to 4-cell stage, cortical beads had only reached the equator when those in untreated siblings had reached the blastoderm (1 hour after injection). An hour later, beads reached the blastoderm, but instead of entering a blastomere they entered the enlarged yolk syncytium. A similar entry of beads only into the syncytium was seen in embryos treated at the 8-cell stage, after injection at the 2-cell to 4-cell stage (Fig. 11g). In contrast, in embryos treated at the 128-cell stage, beads were found not only in the enlarged yolk syncytium, but also in blastomeres (Fig. 11h). This distribution of beads was similar to the distribution in untreated embryos (Fig. 11i).

Discussion

The zebrafish yolk cortex contains dynamic microtubules

Early in development, the cortex of the zebrafish yolk cell contains numerous short microtubules. Microtubules at the vegetal pole transiently form a parallel array in the first cell cycle, while those near the equator have no obvious alignment. The equatorial microtubules increase gradually in length and become aligned in the animal–vegetal axis, and, as early as the 8-cell stage [25], appear continuous between marginal blastomeres and the yolk cytoplasmic layer. There is a reorganization of yolk microtubules, therefore, both in position and in length, indicating that they are dynamic. This is confirmed by their sensitivity to low doses of nocodazole. The change from many short microtubules to fewer long ones, as seen adjacent to the blastoderm, is probably a result of the dynamic instability of microtubules [39]. Dynamic instability alone will not give rise to consistently aligned microtubules, however, and it is likely that the formation of well-aligned arrays also involves the bundling of preexisting microtubules, in the same way as has been proposed for microtubule arrays in axons [40].

Cortical yolk microtubules and specification of the dorsoventral axis

Previous work on several teleost species, such as *Fundulus*, goldfish and *Salmo*, has shown that blastomeres isolated from the yolk cell at early stages form only 'hyperblastulae', whereas those isolated at later stages form axial structures [21,23,35]. The early stage embryos did form axial structures, however, when a portion of the yolk cell was left connected to the blastomeres [23]. With embryos at the 1-cell to 2-cell stage, axial structures formed only when latitudinal cuts were made close to the vegetal pole. With older embryos, the vegetal hemisphere of the yolk cell was not required. This led to the proposal that axis formation in teleosts requires the transfer of substances from the vegetal hemisphere of the yolk cell into the blastoderm [35]. These substances seem to be located in the cortex, as the yolk proper is not absolutely necessary for the formation of axial structures [35]. The data presented here suggest that axis formation in the zebrafish is similarly dependent on the transport of substances from the yolk cell to the blastoderm. Moreover, they suggest that these substances are transported by cortical microtubules.

The experiments with polystyrene beads indicate that substances in the yolk cortex can move from the vegetal hemisphere towards the animal pole and eventually enter marginal blastomeres. Polystyrene beads have been shown to mimic the movement of endogenous organelles in a variety of cell types [36–38], and in the zebrafish yolk cortex they seem to mimic the movement of cytoplasmic granules (at least). Several observations indicate that the movement of beads in the yolk cortex is dependent on microtubules. Firstly, the spread of beads is asymmetric, and is different from the spread of Nile Red or TRITC–dextran, indicating that movement in not simply the result of diffusion. Secondly, the incubation of embryos in nocodazole, at doses that completely depolymerize cortical microtubules, is able to arrest the movement of beads. Thirdly, the movement of the beads is saltatory, as is usually the case for substances propelled along microtubules. Finally, the different behaviour of neighbouring beads indicates that movement is not due to bulk flow of the cytoplasm.

Support for the notion that early blastomeres of the zebrafish do not contain all the molecules necessary for the formation of an axis, but require a substance from the yolk cell, is provided here by the experiments in which cleavage-stage embryos were grown at 18 °C or in 0.1 μg ml^{-1} nocodazole. These treatments cause the premature formation of an enlarged yolk syncytial layer, while blastomeres continue to divide in a pocket at the animal pole. When embryos were treated prior to the 32-cell stage, they failed to translocate β-catenin into nuclei, to express *goosecoid* and *forkhead2*, and to gastrulate. Treatment at later stages did not have these effects. One interpretation of these findings is that the putative determinants normally

enter blastomeres at approximately the 32-cell stage. If embryos are treated with cold or nocodazole at earlier stages, blastomeres become separated from the yolk cortex by the enlarged syncytium and are unable to receive the determinants. This interpretation is supported by the behaviour of beads injected into the vegetal hemisphere: when injected into early-treated embryos, the beads were found later in the syncytial layer only; when injected into late-treated embryos, which have an axis, or into untreated embryos, the beads were found later in both the syncytial layer and blastomeres. This suggests that components of the vegetal hemisphere cortex must enter blastomeres, and not only the yolk syncytial layer, for an axis to form.

The preceding discussion still leaves open the question of how asymmetry is created in the embryo. The present data suggest that the vegetal array of microtubules is involved. UV irradiation of the embryo at early stages prevents formation of the dense array at the vegetal pole, and also prevents formation of the axis. Other microtubule-destabilizing treatments, such as exposure to hydrostatic pressure [41] or a pulse of nocodazole, also lead to defects in the axis when applied to the zygote, indicating that the effects of UV irradiation are not due to the disruption of mRNA. We propose that the vegetal array asymmetrically distributes organelles of the vegetal-pole cortical cytoplasm, as has been documented in medaka [42] and *Xenopus* [43] zygotes. The early asymmetry in the yolk cell that would result from this trafficking is consistent with findings in the goldfish that longitudinal bisections through the first cleavage plane give rise to three classes of embryo: perfect half-sized embryos, embryos with varying axis defects and embryos without any axis [44]. The shallow position of the vegetal array suggests that any asymmetry it creates could subsequently be transferred to the blastoderm by cortical microtubules extending from the marginal blastomeres to the vegetal hemisphere.

Conclusions

Here, we describe the organization of microtubules in the yolk cell of the zebrafish embryo during early development, and provide evidence for their involvement in the specification of the dorsoventral axis. Microtubules in the yolk cortex are dynamic, and form two distinct types of arrays — first, a transient array at vegetal pole, and then longer-lived arrays that apparently extend from marginal blastomeres into the yolk cortex. The second array is able to transport substances from the vegetal hemisphere into marginal blastomeres, and we propose that it acts in axis specification by transporting molecules required for the formation of an axis. Asymmetry may be created in the vegetal hemisphere by the first array of microtubules. Given the amenability of the yolk cell to microinjection and microscopy, and the anticipated availability of maternal-effect mutants, the zebrafish may well be a powerful system for the analysis of the mechanisms that regulate dynamic microtubules *in vivo*, and of their role in the specification of the dorsoventral axis in vertebrates.

Materials and methods

Immunolabelling of microtubules

Embryos were fixed and labelled as described [24], and then mounted and orientated in 70 % glycerol in phosphate-buffered saline (PBS) or in Citifluor (UKC Chemicals). Imaging was carried out with a confocal microscope (BioRad MRC-600). All images are projections of multiple planes, unless otherwise stated. High magnification images in Figure 1 were crispened using the C7C convolution (BioRad).

Quantitation of microtubule length

Lengths of the microtubules were measured using BioRad COMOS software. In embryos in which fibrils/bundles appeared to branch, measurements were made from the apparent tips near the blastoderm to the ends in the yolk cytoplasmic layer, following only one of two possibilities when a branch occurred. Ten different fibrils/bundles were measured per embryo. As the images used were projections of multiple planes of focus, in some cases covering over 100 μm of vertical distance, an approximate correction factor was introduced to compensate for the error caused by the fact that the microtubules were at an angle to the projection plane. The factor used was $\delta = \sqrt{1 + x^2/y^2}$, where x is the vertical height scanned and y is the size of the region imaged, in the direction parallel to the microtubules.

UV irradiation

Embryos obtained by fertilization *in vitro* [26] were UV-irradiated for 90 sec, using a source that provided 4 mW cm^{-2}, as described previously [24].

Nocodazole treatment

The required concentrations were obtained by diluting a stock solution of nocodazole (Sigma; 5 mg ml^{-1} in DMSO) in 5 ml E3 (5 mM NaCl, 0.17 mM KCl, 0.33 mM $CaCl_2$, 0.33 mM $MgSO_4$; [45]). Embryos were placed in these solutions with their chorion intact. For transient treatment, embryos were transferred to the solution of nocodazole, and then through three changes of E3, using a tea-strainer. Treatment times of 2, 4, 6 and 8 min were tested; the latter two times were found to give high lethality. The incubation of embryos in DMSO alone did not give rise to abnormal development.

Cold treatment

Embryos, still in their chorions, were transferred to pre-cooled E3, and then kept in an 18 °C incubator. Note that the minimum temperature for normal development of the zebrafish zygote is 23 °C [46].

In situ *hybridization*

Embryos were fixed in 4 % paraformaldehyde in PBS. Cold-treated embryos were fixed 11.5 h after treatment; nocodazole-treated embryos were fixed when untreated siblings reached 50 % epiboly. Hybridizations with digoxigenin-labelled RNA probes were carried out as described previously [27].

Labelling for β-catenin and Notail

Embryos were fixed in 4 % paraformaldehyde in PBS overnight at 4 °C. After several washes in PBS, embryos were incubated for 1 h in PBS with 1 % BSA and 0.5 % Triton. The primary antibody was used at a dilution of 1:50 for β-catenin [34] or 1:1000 for Notail [29]; the secondary peroxidase-conjugated goat anti-rabbit (Dianova), was used at 1:2 000.

Bead/Nile Red and dextran injection

A suspension of 0.2 μm fluorescent polystyrene beads (1 μ; #17151, Polysciences) was diluted in 23 μl water, together with 1 μl of a Nile Red (Molecular Probes) stock solution (1 μg ml^{-1} in acetone). Dextran coupled to tetramethylrhodamine isothiocyanate (10 000 MW TRITC–dextran; Molecular Probes) was used at a concentration of 100 μg ml^{-1} in water. The bead/Nile Red mixture or dextran was backfilled into pulled capillaries (Clarks; 1.0 mm O.D. with filament) and microinjected into the yolk cell of dechorionated embryos using a gas pressure injector (Eppendorf), near the vegetal pole. As a result of the fragility and distorted morphology of early embryos (of less than 15 min

old) after dechorionation, beads could not be targeted to the vegetal pole of young embryos. At least 10 embryos were injected and analyzed for each treatment. To record the position of beads/Nile Red, embryos were mounted in methyl cellulose and imaged with a confocal microscope using a 10× objective. For the time-lapse analysis of beads, embryos were imaged with an intensified CCD, using a 40× objective. To image cytoplasmic granules, a high-resolution CCD was used, with Nomarski optics and a 40× objective. Images were recorded with a time-lapse video recorder and an OMDR. The displacement of particles was calculated by plotting their position every 3 sec, off a computer screen, and measuring the distance between points.

Acknowledgements

We thank Jörg Ordenthal, Stefan Schulte-Merker, Stefan Schneider, Patrick Blader and Siegfried Roth for probes and antibodies, and Friedrich Bonhoeffer for providing space and facilities. S.J. was supported by EMBO and the Human Frontiers Science Program; U.S. was funded by the Deutsche Forschungsgemeinschaft, INSERM, CNRS, Centre Hospitalier Universitaire Regional, ARC and GREG. We are grateful to colleagues at the MPI and Julian Lewis for reading the manuscript.

References

1. Oppenheimer JM: Transplantation experiments on developing teleosts (***Fundulus*** and ***Perca***). *J Exp Zool* 1936, 72:377–391.
2. Spemann H, Mangold H: Über Induktion von Embryonalanlagen durch Implantation artfremder Organisatoren. *Roux's Arch Dev Biol* 1924, 100:599–638.
3. Waddington CH: Experiments on the development of the chick and duck embryo cultivated ***in vitro***. *Proc Trans R Soc Lond (B)* 1932, 211:179–230.
4. Beddington RSP: Induction of a second neural axis by the mouse node. *Development* 1994, 120:613–620.
5. Ancel P, Vintemberger P: Recherches sur le detérminisme de la symetrie bilatérale dans l'oeuf des Amphibiens. *Bull Biol Fr Belg* 1948, 31(Suppl):1–182.
6. Vincent J-P, Oster GF, Gerhart JC: Kinematics of grey crescent formation in ***Xenopus*** eggs: the displacement of subcortical cytoplasm relative to the egg surface. *Dev Biol* 1986, 113:484–500.
7. Ho R: Axis formation in the embryo of the zebrafish ***Brachydanio rerio***. *Semin Dev Biol* 1992, 3:53–64.
8. Kimmel CB, Warga RM: Indeterminate cell lineage of the zebrafish embryo. *Dev Biol* 1987, 124:269–280.
9. Abdelilah S, Solnica-Krezel L, Stainier DYR, Driever W: Implications for dorsoventral axis determination from the zebrafish mutation ***janus***. *Nature* 1994, 370:468–471.
10. Helde KA, Wilson ET, Cretekos CJ, Grunwald DJ: Contribution of early cells to the fate map of the zebrafish gastrula. *Science* 1994, 265:517–520.
11. Wacker S, Herrmann K, Berking S: The orientation of the dorsal–ventral axis of zebrafish is influenced by gravitation. *Roux's Arch Dev Biol* 1994, 203:281–283.
12. Clapp CM: Some points in the development of the toad-fish (***Batrachus tau***). *J Morphol* 1891, 5:494–501.
13. Oppenheimer JM: Processes of localization in developing ***Fundulus***. *J Exp Zool* 1936, 73:405–444.
14. Morgan TH: The formation of the fish embryo. *J Morphol* 1895, 10:419–472.
15. Hoadley L: On the localization of the developmental potencies in the embryo of ***Fundulus heteroclitus.*** *J Exp Zool* 1928, 227:7–44.
16. Schmitz B, Campos-Ortega JA: Dorso-ventral polarity of the zebrafish embryo is distinguishable prior to the onset of gastrulation. *Roux's Arch Dev Biol* 1994, 203:374–380.
17. Stachel SE, Grunwald DJ, Myers PZ: Lithium perturbation and goosecoid expression identify a dorsal specification pathway in pregastrula zebrafish. *Development* 1993, 117:1261–1274.
18. Dirksen M-L, Jamrich M: Differential expression of ***forkhead*** genes during early ***Xenopus*** and zebrafish development. *Dev Genet* 1995, 17:107–116.
19. Berridge MJ, Downes CP, Hanley MR: Neural and developmental actions of lithium: a unifying hypothesis. *Cell* 1989, 59:411–419.
20. Klein PS, Melton DA: A molecular mechanism for the effect of lithium on development. *Proc Natl Acad Sci USA* 1996, 93:8455–8459.
21. Oppenheimer JM: The development of isolated blastoderms of ***Fundulus heteroclitus.*** *J Exp Zool* 1936, 72:247–269.
22. Kostomarova AA: The differentiation capacity of isolated loach (***Misgurnis fossilis*** L.) blastoderm. *J Embryol Exp Morphol* 1969, 22:407–430.
23. Tung TC, Chang CY, Tung YFY: Experiments on the developmental potencies of blastoderms and fragments of teleostean eggs separated latitudinally. *Proc Zool Soc Lond* 1945, 115:175–188.
24. Strähle U, Jesuthasan S: Ultraviolet irradiation impairs epiboly in zebrafish embryos: evidence for a microtubule-dependent mechanism of epiboly. *Development* 1993, 119:909–919.
25. Solnica-Krezel L, Driever W: Microtubule arrays of the zebrafish yolk cell: organization and function during epiboly. *Development* 1994, 120:2443–2455.
26. Westerfield M (ed.). *The Zebrafish Book*, 2nd edn. Eugene, Oregon: University of Oregon Press; 1993.
27. Strähle U, Blader P, Henrique D, Ingham PW: ***Axial***, a zebrafish gene expressed along the developing body axis, shows altered expression in ***cyclops*** mutant embryos. *Genes Dev* 1993, 7:1436–1446.
28. Krauss S, Concordet J-P, Ingham PW: A functionally conserved homolog of the ***Drosophila*** segment polarity gene ***hedgehog*** is expressed in tissues with polarizing activity in zebrafish embryos. *Cell* 1993, 75:1431–1444.
29. Schulte-Merker S, Ho RK, Hermann BG, Nüsslein-Volhard C: The protein product of the zebrafish homologue of the mouse T gene is expressed in nuclei of the germ ring and the notochord of the early embryo. *Development* 1992, 116:1021–1032.
30. Hoebeke J, Van Nigen G, De Brabander M: Interactions of nocodazole (R17934), a new antitumoral drug, with rat brain tubulin. *Biochem Biophys Res Commun* 1976, 69:319–342.
31. Lee JC, Field DJ, Lee LLY: Effects of nocodazole on structure of calf brain tubulin. *Biochemistry* 1980, 19:6209–6215.
32. Tilney LG, Porter KR: Studies on the microtubules in helioza. II The effects of low temperature of these structures in the formation and maintenance of the axopodia. *J Cell Biol* 1967, 34:327–343.
33. Weisenberg RC: Microtubule formation ***in vitro*** in solutions containing low calcium concentrations. *Science* 1972, 177:1104–05.
34. Schneider S, Steinbesser H, Warga R, Hausen P: β-catenin translocation into nuclei demarcates the dorsalising centers in frog and fish embryos. *Mech Dev* 1996, 57:191–198.
35. Devillers C: Structural and dynamic aspects of the development of the teleostean egg. *Adv Morphol* 1961, 1:379–428.
36. Adams RJ, Bray D: Rapid transport of foreign particles microinjected into crab axons. *Nature* 1983, 303:718–720.
37. Beckerle MC: Microinjected fluorescent polysterene beads exhibit saltatory motion in tissue culture cells. *J Cell Biol* 1984, 98:2126–2132.
38. Hamaguchi MS, Hamaguchi Y, Hiramoto Y: Microinjected polysterene beads move along astral rays in sand dollar eggs. *Dev Growth Differ* 1986, 28:461–470.
39. Mitchison TJ, Kirschner M: Dynamic instability of microtubule growth. *Nature* 1984, 312:237–242.
40. Joshi HC, Baas PW: A new perspective on microtubules and axon growth. *J Cell Biol* 1993, 121:1191–1196.
41. Hatta K, Kimmel CB: Midline structures and CNS coordinates in zebrafish. *Perspect Neu Dev* 1993, 1:257–268.
42. Timble LM, Fluck RA: Indicators of the dorsoventral axis in medaka (***Oryzias latipes***) zygotes. *Fish Biol J* 1995, 7:37–41.
43. Rowning BA, Wells JC, Gerhart JC, Larabell CA: Microtubule-mediated transport of organelles toward the prospective dorsal side of ***Xenopus*** eggs. *Mol Biol Cell* 1995, 6:345a.
44. Tung TC, Tung YFY: Experimental studies on the development of goldfish. *Proc Chin Physiol Soc* 1943, 2:11–12.
45. Haffter P, Granato M, Brand M, Mullins MC, Hammerschimdt M, Kane DA, *et al.*: The identification of genes with unique and essential functions in the development of the zebrafish, ***Danio rerio***. *Development* 1996, 123:1–36.
46. Schirone RC, Gross L: Effect of temperature on early embryological development of the zebrafish, ***Brachydanio rerio***. *J Exp Zool* 1968, 169:43–52.
47. Greenspan P, Mayer EP, Fowler SD: Nile Red: a selective fluorescent stain for intracellular lipid droplets. *J Cell Biol* 1985, 100:965–973.